

# REPORT

SAND2007-6324

Unlimited Release

Printed October 2007

## Demonstration of the Self-Magnetic-Pinch Diode as an X-ray Source for Flash Core-Punch Radiography

Salvador Portillo, Bryan V. Oliver, Steve R. Cordova, Nichelle Bruner, Derek Ziska, Dean Rovang

Prepared by  
Sandia National Laboratories  
Albuquerque, New Mexico 87185 and Livermore, California 94550

Sandia is a multiprogram laboratory operated by Sandia Corporation, a Lockheed Martin Company, for the United States Department of Energy's National Nuclear Security Administration under Contract DE-AC04-94AL85000.

Approved for public release; further dissemination unlimited.

Issued by Sandia National Laboratories, operated for the United States Department of Energy by Sandia Corporation.

**NOTICE:** This report was prepared as an account of work sponsored by an agency of the United States Government. Neither the United States Government, nor any agency thereof, nor any of their employees, nor any of their contractors, subcontractors, or their employees, make any warranty, express or implied, or assume any legal liability or responsibility for the accuracy, completeness, or usefulness of any information, apparatus, product, or process disclosed, or represent that its use would not infringe privately owned rights. Reference herein to any specific commercial product, process, or service by trade name, trademark, manufacturer, or otherwise, does not necessarily constitute or imply its endorsement, recommendation, or favoring by the United States Government, any agency thereof, or any of their contractors or subcontractors. The views and opinions expressed herein do not necessarily state or reflect those of the United States Government, any agency thereof, or any of their contractors.

Printed in the United States of America. This report has been reproduced directly from the best available copy.

Available to DOE and DOE contractors from  
U.S. Department of Energy  
Office of Scientific and Technical Information  
P.O. Box 62  
Oak Ridge, TN 37831

Telephone: (865) 576-8401  
Facsimile: (865) 576-5728  
E-Mail: [reports@adonis.osti.gov](mailto:reports@adonis.osti.gov)  
Online ordering: <http://www.osti.gov/bridge>

Available to the public from  
U.S. Department of Commerce  
National Technical Information Service  
5285 Port Royal Rd.  
Springfield, VA 22161

Telephone: (800) 553-6847  
Facsimile: (703) 605-6900  
E-Mail: [orders@ntis.fedworld.gov](mailto:orders@ntis.fedworld.gov)  
Online order: <http://www.ntis.gov/help/ordermethods.asp?loc=7-4-0#online>



# Demonstration of the Self-Magnetic-Pinch Diode as an X-ray Source for Flash Core-Punch Radiography

S. Portillo<sup>1</sup>, B. V. Oliver<sup>1</sup>, S. R. Cordova<sup>1</sup>, D. Rovang<sup>1</sup>, N. Bruner<sup>2</sup> and D. Ziska<sup>3</sup>  
*Sandia National Laboratories*  
*P.O. Box 5800*  
*Albuquerque, New Mexico 87185*

## Abstract

Minimization of the radiographic spot size and maximization of the radiation dose is a continuing long-range goal for development of electron beam driven X-ray radiography sources. In collaboration with members of the Atomic Weapons Establishment(AWE), Aldermaston UK , the Advanced Radiographic Technologies Dept. 1645 is conducting research on the development of X-ray sources for flash core-punch radiography. The Hydrodynamics Dept. at AWE has defined a near term radiographic source requirement for scaled core-punch experiments to be 250 rads@m with a 2.75 mm source spot-size. As part of this collaborative effort, Dept. 1645 is investigating the potential of the Self-Magnetic-Pinched (SMP) diode as a source for core-punch radiography. Recent experiments conducted on the RITS-6 accelerator [1,2] demonstrated the potential of the SMP diode by meeting and exceeding the near term radiographic requirements established by AWE. During the demonstration experiments, RITS-6 was configured with a low-impedance (40  $\Omega$ ) Magnetically Insulated Transmission Line (MITL), which provided a 75-ns, 180-kA, 7.5-MeV forward going electrical pulse to the diode. The use of a low-impedance MITL enabled greater power coupling to the SMP diode and thus allowed for increased radiation output. In addition to reconfiguring the driver (accelerator), geometric changes to the diode were also performed which allowed for an increase in dose production without sacrificing the time integrated spot characteristics. The combination of changes to both the pulsed power driver and the diode significantly increased the source x-ray intensity.

<sup>1</sup>Email: [sportil@sandia.gov](mailto:sportil@sandia.gov)

<sup>2</sup>Permanent address: Voss Scientific, Albuquerque, New Mexico.

<sup>3</sup>Permanent address: K-Tech Corporation, Albuquerque, New Mexico.

## **Acknowledgements**

The authors acknowledge Mr. Isidro Molina (SNL) for his technical expertise and operational support on RITS-6 and Dr. Paul L. Mix (SNL) for help with programming software necessary for data analysis. We also thank the RITS-6 crew for their support in fielding these experiments, Mr. Ray Gignac and Mr. Frank Wilkins of the NSTec corporation and Mr. Toby Romero of K-Tech corporation. Valuable technical discussions were conducted with Jim Threadgold, Aled Jones, Ian Crotch and John O'Malley of the Atomic Weapons Establishment, David Hinshelwood of the Naval Research Laboratory and Dale Welch of Voss Scientific.

Sandia is a multiprogram laboratory operated by Sandia Corporation, a Lockheed-Martin company, for the United States Department of Energy's National Nuclear Security Administration, under contract DE-AC04-94AL85000.

## Contents

I.	Introduction.....	6
II.	Experimental Configuration.....	8
	A. Low Impedance Configuration for RITS-6 .....	8
	B. Electrical Diagnostics .....	9
	C. Dosimetry and Spot Size Diagnostics .....	10
III.	Results.....	12
IV.	Conclusions.....	18
	References.....	19

## Figures

1a.	Illustration of the RITS-6 accelerator .....	7
1b.	Illustration of the MITL and diode region .....	7
2.	Illustration of the SMP diode.....	8
3.	Electrical signals for RITS-6 MITL and SMP diode. ....	10
4.	Cross section of RITS-6 test cell and locations of diagnostics.....	11
5.	Penumbral measurement technique for measuring spot size .....	12
6.	Electrical characteristics of an SMP diode .....	13
7.	Comparison of diode voltage calculations.....	14
8.	Comparison of dose rate output for low and high Impedance MITL driven SMP.....	15
9.	Comparison of LSF and ESF spot size smp diode .....	15
10.	2 dimensional reconstruction of beam profile.....	16
11.	Spot size and dose plot for SMP cathode series .....	17

## I. Introduction

In collaboration with members of the Atomic Weapons Establishment (AWE), the Advanced Radiographic Technologies Dept. 1645 is conducting research on the development of X-ray sources for flash core-punch radiography. The source development is conducted on the Radiographic Integrated Test Stand (RITS-6) [1,2].

RITS-6 is an Inductive Voltage Adder (IVA) accelerator developed at Sandia National Laboratories for driving high brightness flash x-ray radiographic sources. In its present configuration six induction cells are each driven by an  $8\Omega$  parallel water dielectric pulse forming line. The individual induction cells are joined in series by a vacuum coaxial Magnetically Insulated Transmission Line (MITL) which delivers power from the cells to a diode region, where the electron beam is created. The geometry of the accelerator and diode region is shown in Fig. 1a. It is capable of delivering greater than 10-MV, 125-kA, 75-ns pulses to high impedance ( $> 200\ \Omega$ ) electron beam diodes. Flexibility in the architecture via changes to the MITL operating point and or geometry also allows for the ability to deliver  $\sim 7.5$ -MV, 180-kA, 75-ns pulses to lower impedance ( $\sim 50\ \Omega$ ) diodes.

A field shaping “knob” is attached (Fig. 1b) at the end of the MITL, just upstream of the diode anode-cathode (A-K) gap. The knob serves to shed excess flow current from the MITL and shield accelerator components from debris generated by the diode. In the diode region, the electron beam is generated at the cathode, accelerated across the A-K gap and impinges the anode. The anode is usually a  $1/3$  electron-range thick high atomic number ( $Z$ ) target (e.g. Tantalum) The stopping of the e-beam in the anode/target generates bremsstrahlung radiation. The radiation is extracted in the forward direction and used for imaging dense material via point projection X-ray radiography.

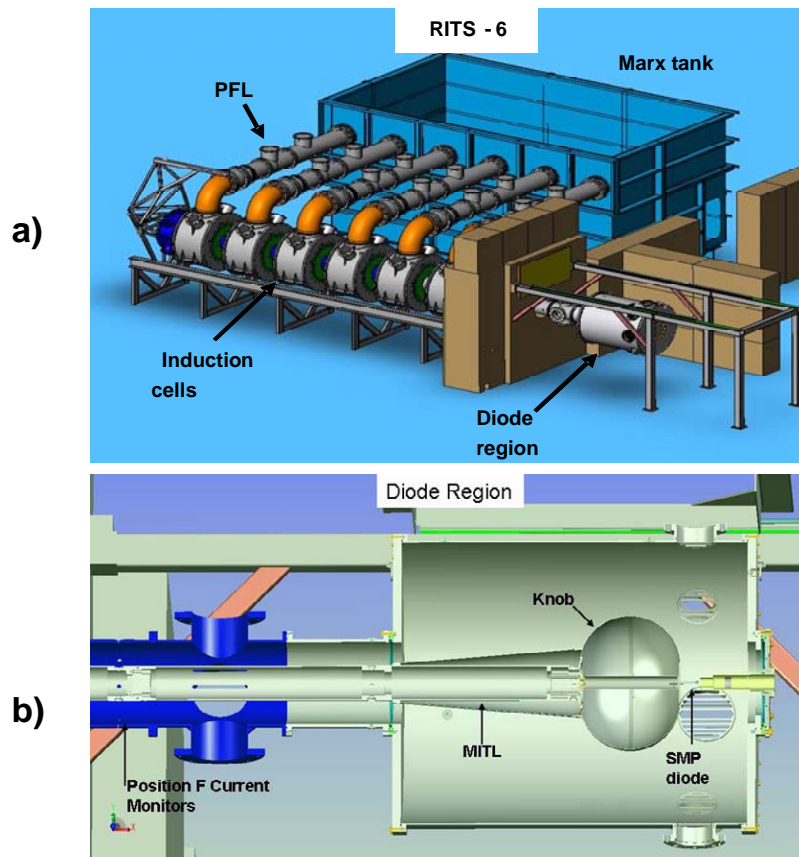


Figure 1. Illustration of a) the RITS-6 accelerator and b) a cutaway of the MITL and diode region.

Minimization of the radiographic spot size and maximization of the radiation dose is a long-range goal for development of electron beam driven X-ray radiographic sources. A near term radiographic source requirement for scaled core-punch experiments is 250 rads@m with a 2.75 mm source spot-size [3]. As part of a collaborative effort with the Atomic Weapons Establishment, Sandia National Labs is evaluating the Self-Magnetic-Pinched (SMP) diode [4] as a possible source to meet both near-term and long-range radiography requirements. The SMP diode consists of an anode and hollow cathode separated by a small A-K gap typically on the order of 1 cm. The anode is comprised of a thin Al foil and a converter made of Ta. The foil and Ta converter are typically separated by a small vacuum gap. Electrons emitted from the cathode are accelerated across the A-K gap and impinge the anode within a diameter that is larger than the cathode diameter. As the current in the diode increases, the electrons heat the anode foil and eventually cause ions to emit from the anode surface (typically within  $\sim 5$ -10 ns after the beginning of electron emission). The ions are accelerated across the A-K gap and provide nearly complete charge neutralization of the electron beam. This results in both an increased diode current (due to enhanced space-charge limited emission of the electrons from the cathode and

a contribution due to the ion current) and a pinching of the electron beam due to the self-magnetic field generated in the diode. Because of the cylindrical geometry, the magnetic field is expected to be azimuthally symmetric and can thus efficiently compress the beam by a factor of nearly 5 upon traversing the A-K gap, resulting in e-beam diameters on target significantly smaller than the cathode diameter and of order 2-3 mm.

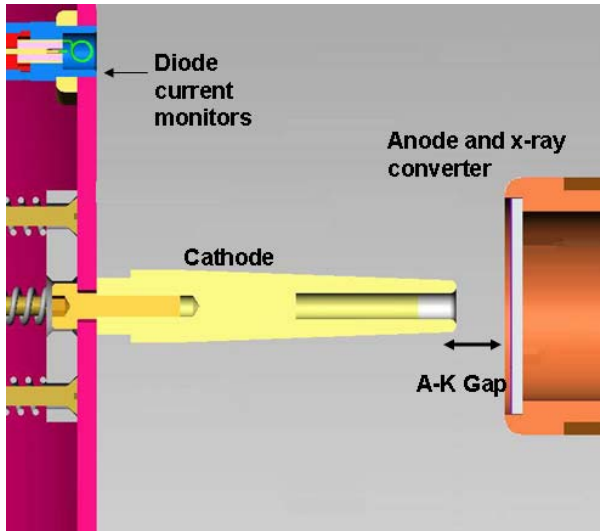


Figure 2. Illustration of the SMP diode

The results presented here demonstrate the potential of the SMP diode as a future high brightness source by meeting and exceeding the near term radiographic requirements established by AWE. During these experiments, RITS-6 was configured with a low-impedance ( $\sim 40 \Omega$ ) MITL, the use of which enabled greater power coupling to the SMP diode and thus allowed for increased radiation output. In addition to reconfiguring the driver (accelerator), geometric changes to the diode were also performed which allowed for an increase in dose production without sacrificing the time integrated spot characteristics. The combination of changes to both the pulsed power driver and the diode significantly increased the source X-ray intensity.

## II. Experimental Configuration

### A. Low Impedance Configuration for RITS-6

The nominal configuration for RITS-6 is a high impedance mode capable of delivering a greater than 10-MV, 120-kA forward going wave to the diode region. In this mode, the induction cores are threaded by a MITL with a characteristic operating impedance of about  $80 \Omega$ , which is optimal for driving high impedance ( $\sim 200 \Omega$ ) diodes such as the Paraxial diode [5] and the Immersed-Bz diode [6]. On previous studies the SMP diode was characterized using RITS-6 in the high impedance configuration. In this and other related studies [ref. Hinshelwood and Threadgold] it was determined that the diode has a

characteristic impedance that begins around 40-50  $\Omega$  and falls to ~20-30  $\Omega$  during the pulse. Because of this, the SMP diode is not well-matched to the nominal RITS-6 configuration.

Numerical studies of the operating characteristics of IVA's [7,8] demonstrate the possibility of operating the accelerator in a low impedance mode by under-matching the MITL to the accelerator induction cells. For particular MITL geometries, this can be accomplished without significantly degrading the forward power to the diode region. We have therefore designed and threaded the RITS-6 cores with a low-impedance (40- $\Omega$ ) MITL which provides a 75-ns full-width-half-maximum (FWHM), 180-kA, 7.5-MV forward going electrical pulse to the diode.

## B. Electrical diagnostics

The accelerator and diode currents are measured with B-dot current monitors at the locations shown in Fig. 1b. The inner (cathode) current,  $I_c$ , and outer (anode)  $I_a$  currents measured at Position F are averaged from 4 discreet B-dot monitors located at 90 degree increments in azimuth. The difference between  $I_a$  and  $I_c$  is the free electron current flowing along the MITL. Based on the theory of Mendel [9], the MITL voltage can be calculated as a function of the anode and cathode currents:

$$V = Z_0 * (I_a^2 - I_c^2)^{1/2} - .511 * \left[ \left( \frac{I_a}{I_c} \right) - 1 \right] * \left[ \left[ 2 \left( \frac{I_a}{I_c} + 1 \right) \right]^{1/2} - 1 \right] \quad (1)$$

where V (MV) is the MITL voltage in MV,  $Z_0=51.3$  is the vacuum impedance of the MITL in Ohms, and  $I_a$  and  $I_c$  are expressed in MA. The diode currents are averaged from two B-dot monitors located at the radial position shown in Fig. 2 and separated azimuthally by 90 degrees. Representative accelerator currents at position F, the diode current and calculated voltage at F (based on Eq. 1) for a typical SMP diode shot are shown in Fig. 3. In the low-impedance configuration, the accelerator delivers a forward-going wave with a peak voltage of ~ 7.8 MV and a peak total (anode) current of ~ 185 kA with a pulse width of ~ 70 ns.

The measured diode current rises quickly to ~ 100 kA and then continues to increase at a fairly steady rate to a peak current of ~ 150 kA, suggesting a decreasing diode impedance. A further indication of a falling diode impedance is the presence of a retrapping wave propagating up the MITL and evidenced by the rise in cathode current  $I_c$  from 60 kA to 90 kA, late in the pulse at the position F (in the limit  $I_a = I_c$  the diode impedance tends to zero). The retrapping wave is generated when the diode impedance falls below the characteristic operating impedance of the MITL.

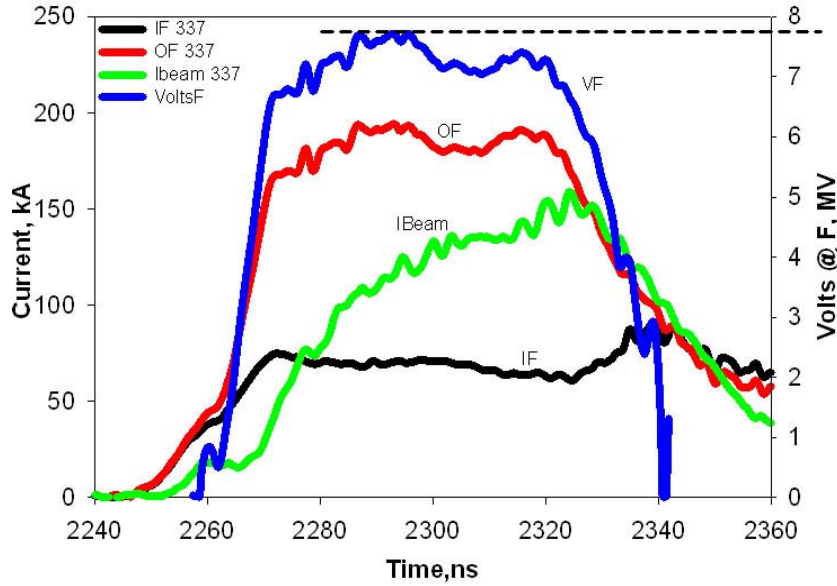


Figure 3 Electrical signals for a typical SMP shot on RITS-6. The cathode current (black) and anode current (red) at position F on the MITL. The Mendel derived voltage (blue) and the diode current (green).

### C. Dosimetry and spot-size diagnostics

Figure 4 shows a layout of the RITS-6 test cell and the location of the dosimetry and spot-size diagnostics used in these experiments. The dosimetry diagnostics are located inside and outside the test cell (at the end of the radiographic aperture shown in Fig. 4). Time-integrated dosimetry measurements are made with equilibrated  $\text{CaF}_2$  thermoluminescent dosimeters (TLDs). Dose rate measurements are made using Si PIN diodes. These PIN signals are cross calibrated to the TLDs to yield an absolute measurement. Although dosimetry is located at various distances from the source, all the dosimetry data (both time-integrated and time-resolved) presented are normalized to the dose equivalent at 1 m, assuming an inverse distance squared scaling. There is the equivalent of 16 mm of aluminum filtering/attenuation between the source and the dose diagnostics.

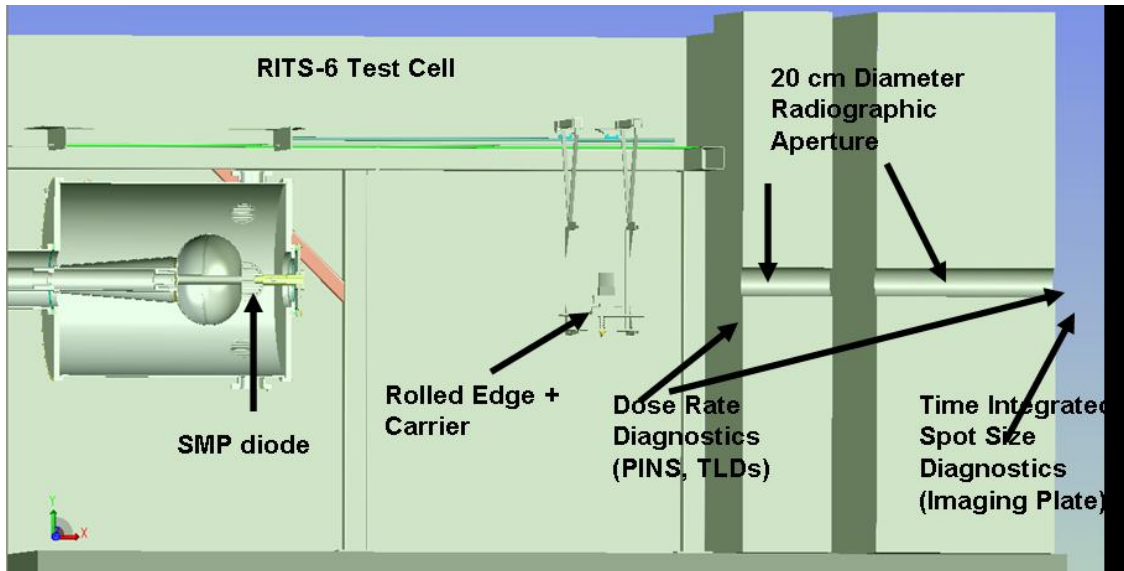


Figure 4. Cross section of the RITS-6 test cell, showing location of the rolled edge and radiation and spot diagnostics.

Spot size measurements of the beam are taken with a tungsten “Rolled Edge”, which is opaque to the incoming radiation and is placed orthogonal to the source. The resulting penumbra is captured on an radiographic Imaging-Plate (IP) detector. The rolled edge and imaging plate were located at the positions shown in Fig. 4. The imaging plate is placed parallel to the rolled edge in a geometry that minimizes blur from the detector as shown in Fig. 5. The resulting penumbral measurement yields the Edge Spread Function (ESF) (see Fig. 5) and by analyzing this transition the spot size can be calculated using various methods. One of the methods we use is the AWE method for determining spot-size[10]. In practice, we use a dual sided rolled edge and thus obtain 2-d radiographic spot information. The AWE method of calculating the spot takes the distance between the 25% and 75% points on the normalized ESF, divided by the magnification, and multiplied by 2.5. This definition yields the equivalent diameter of a uniformly illuminated disk. The derivative of the ESF yields the Line Spread Function (LSF). The LSF can also used to calculate the source spot size. Our method of calculating the spot from the LSF is based on a variant of a Lawrence Livermore (LLNL) method. We define the spot as 1.4 times the FWHM of the LSF. In this case, if the source distribution were Gaussian, the value determined by the AWE definition and the LLNL definition would be equivalent.

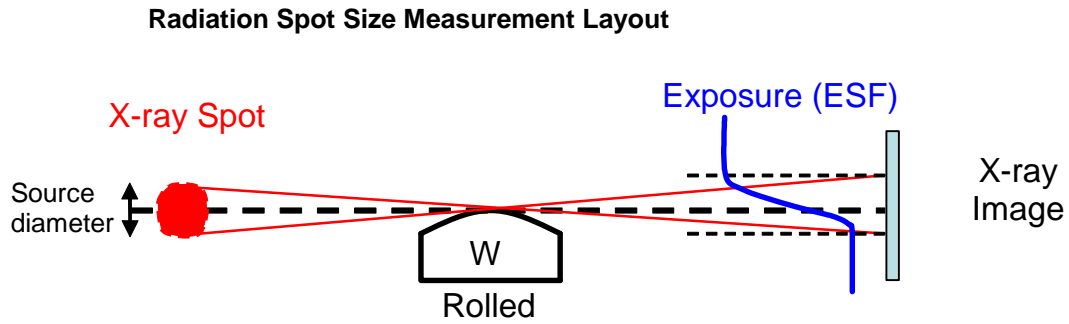


Figure 5 Penumbral measurement technique for measuring spot size.

By having a co-planar 2-dimensional rolled edge it is possible to use the corner where the two edges meet to derive the spot distribution by using the method of Barnea [11,12]. The method calls for taking derivatives of multiple line profiles at every corner of a four corner aperture. We have implemented a modified version of Barnea's methodology for a single corner and present results of spot size measurements in comparison with the standard penumbral-edge technique.

### III. Results

Figure 6 shows typical electrical characteristics for an SMP diode shot and the absolute dose rate measurement from a PIN detector. The radiation pulse width (FWHM) is approximately 46 ns with a peak dose rate of 8 rads/ns at the peak of the diode current. Although the validity of the techniques described above for calculating the voltage in the MITL region are well documented, applying this method to the diode region is problematic because of the lack of an established equilibrium for the electron flow in this region. However, three separate methods for determining the diode voltage are compared and yield reasonable estimates of the actual diode. At present, no direct electron beam energy diagnostic is available with which to more accurately measure the actual voltage. The first method makes use of a radiographer's equation. A radiographer's equation (or dose rate model) which gives the relationship between beam current, diode voltage and the radiation output has been developed by Crotch [13] for the SMP diode and is given by the expression:

$$\frac{dD}{dt} = I_e * [-2.952 * V + 2.349 * V^2 - 0.06934 * V^3] \quad (2)$$

where  $dD/dt$  (rads/ns) is the dose rate,  $I_e$  is the electron beam current impinging on the target in MA, and  $V$  is the time-dependent diode voltage in MV. This equation assumes that the electron beam impinging the anode can be well represented by a 40 degree fully filled cone. This agrees well with the electron trajectories calculated from numerical Particle-In-Cell (PIC) simulations. A radiation transport code is used to propagate the electrons through the target material as well as creating and propagating the resultant bremsstrahlung radiation onto a plane where the energy deposition is measured.

Because the measured diode current includes both electrons and ions, an estimate of the ion current is subtracted from the measured current before using Eq. (2) to solve for the voltage. Based on PIC simulations of the diode, the ion current accounts for ~10% of the total current (independent measurement of the ion current is a present area of research). The current shown in Fig. 6 includes this adjustment. Using the measured dose rate and adjusted beam current, the time dependent diode voltage can be calculated by inverting Eq. (2). The result from such a calculation is shown in Fig. 6 (black line) and labeled  $V_{diode}$ . The diode impedance (blue line) shows that initially there is a fast decaying impedance that stabilizes ~10 ns into the pulse at ~55  $\Omega$ . Once this stable period is over, 10 ns later, the impedance begins a gradual decrease until the end of the radiation pulse to a value of approximately 30  $\Omega$ .

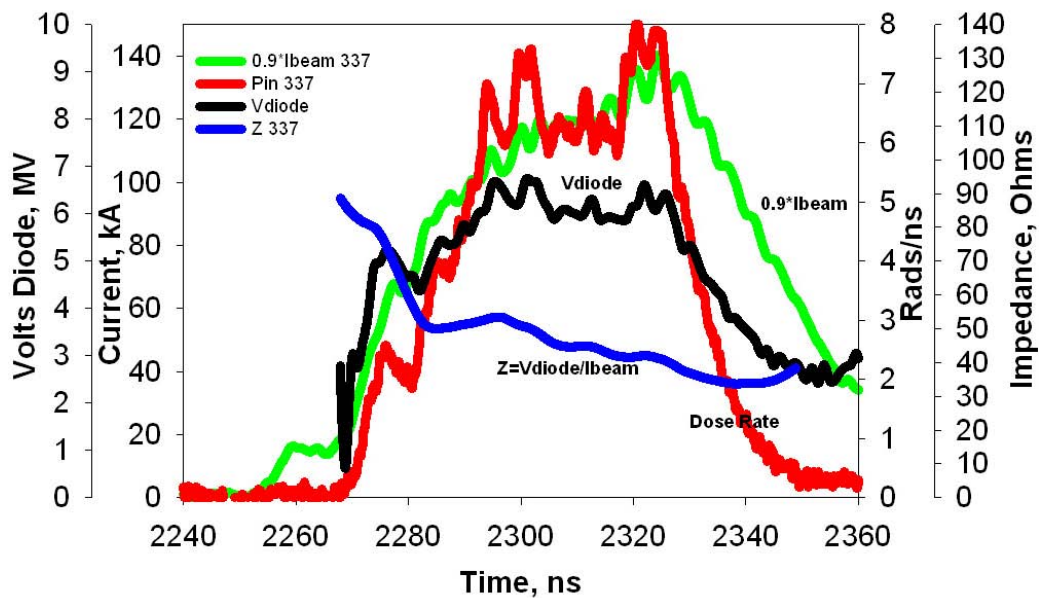


Figure 6. The voltage (black),  $0.9 \times$  diode current (green) and impedance (blue) of the SMP diode on shot 337. Also plotted is the dose rate (red), normalized to dose at a meter.

A second method for estimating the diode voltage uses the measured currents at the position F location on the MITL. As discussed above, provided the MITL is not undergoing rapid impedance changes, it is possible to calculate the voltages by means of the Mendel equation if the cathode and anode currents are known. This is possible at position F for most of the pulse duration since a rapid change in the cathode current is not observed until late in the pulse. By carrying out a finite difference inductive correction to the MITL voltage at position F [14] and by including a lumped-inductive voltage correction for the knob and diode region, the voltage at the diode is estimated. A third method based on PIC simulations [15] is employed to help interpret the experimentally-based estimates. The simulations include the MITL region upstream of the diode (beginning at position F) and include a circuit model with a time dependent impedance to emulate the diode load. The simulations use the calculated forward voltage at position F as input to simulation domain. Comparison of the anode and cathode currents at position F to the simulations confirm the input drive for the simulation. The voltage in the diode

is calculated from the simulation and compared to the voltages based on the radiographer's equation as well as the transmission line corrected voltage from position F. A comparison of the three methods is shown in Fig. 7 for shot 290. Shot 290 had a similar SMP diode configuration (i.e. cathode size and AK gap) to that used on shot 337. The voltage based on the radiographer's equation and the voltage from numerical simulation have very similar shapes (width and amplitude), with the voltage calculated from the simulations suggesting a higher value early in time. The inductively corrected voltage (black line) is also in reasonable agreement for the first 50ns of the pulse, thereafter, however, the method slightly overestimates the voltage.

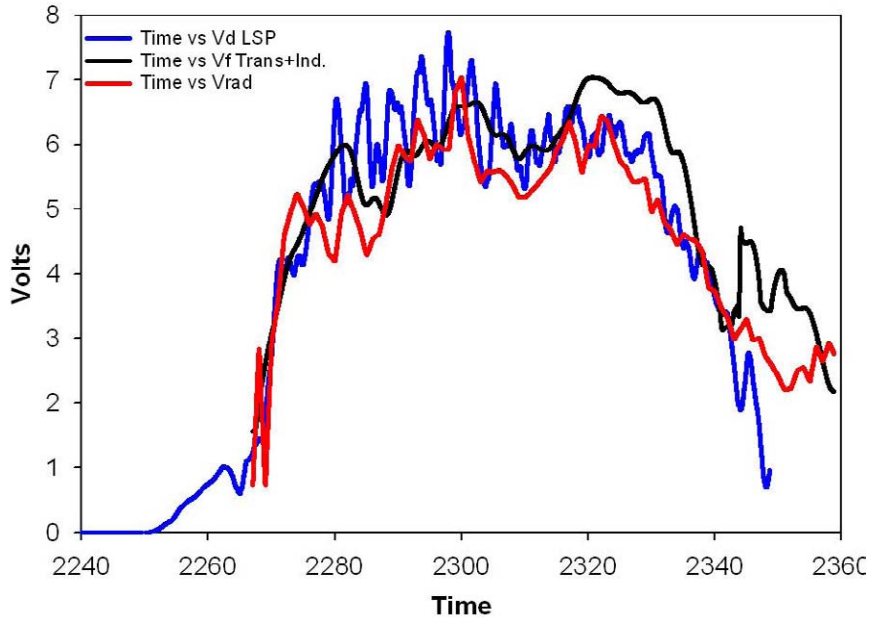


Figure 7. Comparison of three diode voltage calculations for the SMP diode: PIC simulation (blue), radiographer Eq. 2 (red) and inductive correction of Mendel voltage at F (black).

As noted in Sec II A., for these experiments the RITS-6 accelerator is configured with a low impedance MITL in order to better couple the driver to the diode. The improved power-coupling provides a significant improvement in the dose production as shown in Fig. 8. Increases in radiation pulse-width and amplitude resulted in a 74% increase in dose output (203 rads vs. 354 rads). We emphasize for the reader the importance of matching the pulsed power driver to the diode and that the IVA accelerator architecture is flexible enough to accommodate such changes with relatively low cost modifications.

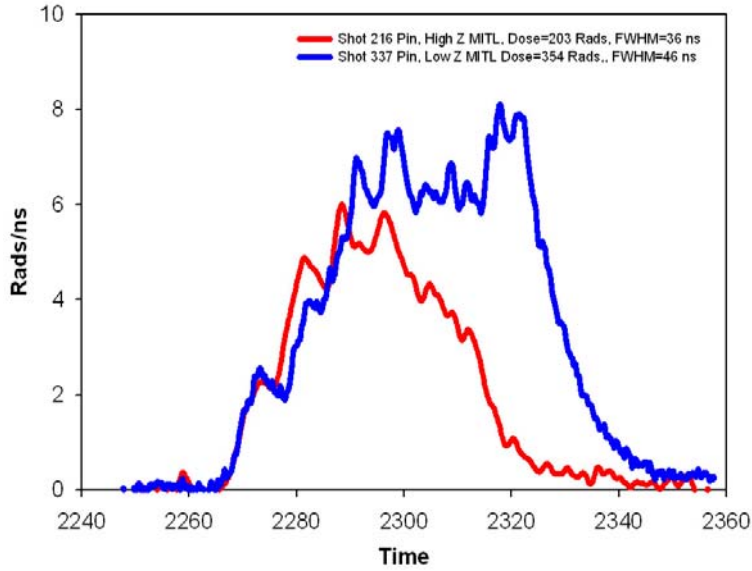


Figure 8 Comparison of the SMP diode radiation output dose rate (rads/ns at 1 meter) for a shot with the low impedance MITL (blue) and a high impedance MITL (red).

In Figure 9 the edge spread function (ESF) and associated line spread function (LSF) measured across the horizontal edge for shot 337 are shown. Analysis of the horizontal edge yields an AWE spot-size definition of 2.4 mm. The LSF-based spot-size definition is 2.2 mm (1.4 times the FWHM of the LSF). For every shot, the spot-sizes determined from the horizontal edge and vertical edge are averaged using the quadratic mean (i.e. square root of the quantity equal to the sum of the values squared divided by two).

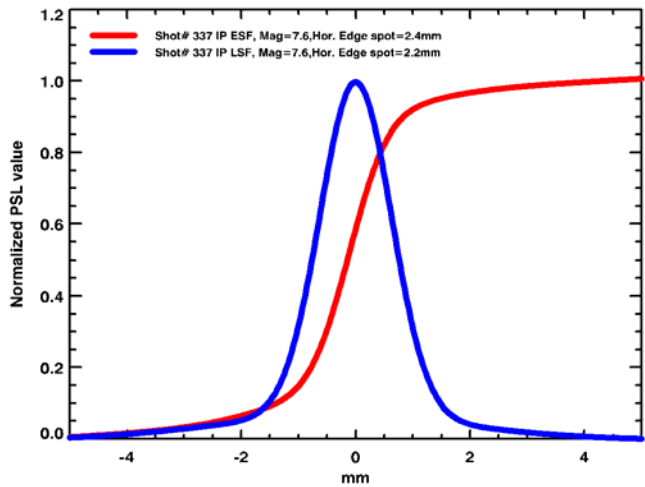


Figure 9. Horizontal-edge ESF (red) and LSF (blue) for shot 337.

The difference between the horizontal and vertical edge spot sizes gives some indication of the relative symmetry of the source. Another way to assess the source symmetry is to

reconstruct a 2-d beam image of the source using the Barnea method. A reconstruction of the source profile using the modified method of Barnea is shown in Fig. 10. The hot core is evident as is a 10% asymmetry in the horizontal and vertical spot sizes.

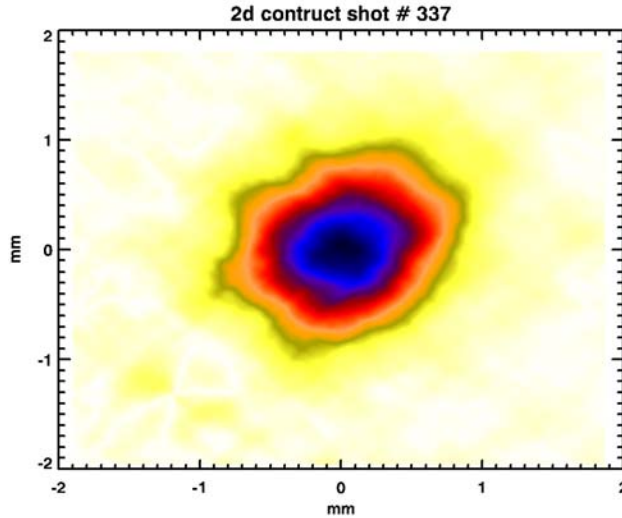


Figure 10. Reconstruction of the beam profile for shot 337.

Results from the experimental campaign which demonstrated optimal x-ray performance, which included shot 337, are summarized in Fig. 12. The dose (rads@m) and spot-size (mm) are plotted for a number of different shots conducted during the experiment. The doses are indicated by the red circles in Fig. 12 and represent the average of two TLD readings at the position where the spot information is recorded. The error bars reflect the absolute variation about the average. The results are given for three separate diode configurations, which can be correlated with the cathode diameter: 8.5 mm (small), 12.5 mm (medium) and 16.5 mm (large). The largest recorded doses occurred for the “medium” cathode diameters, with doses of  $\sim 350$  rads@m being repeated for multiple shots. Peak doses of  $\sim 400$  rads@m were also recorded for the “medium” cathode diode configuration (shots 333 and 334), however these shots were conducted without the rolled-edge in place to make spot-size measurements and thus we can not quantify the complete radiographic utility of those shots.

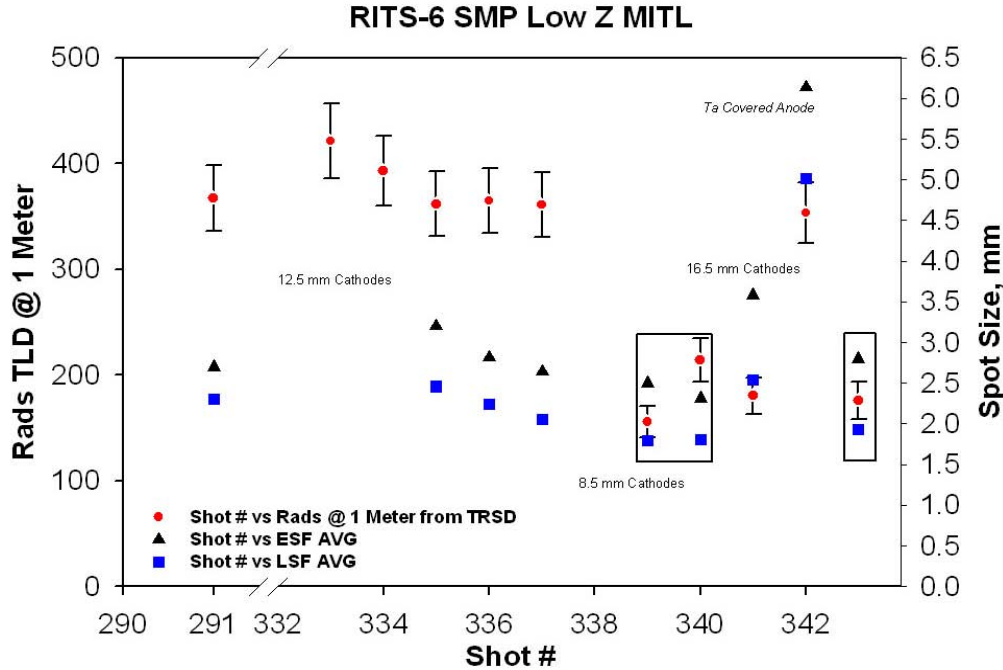


Figure 11. Spot size and dose @ 1 meter for the SMP cathode fielded on RITS-6

The two definitions of the time integrated radiographic source spot-size are indicated in Fig. 11 (blue squares and black triangles). The black triangles represent the AWE definition and the blue squares represent the LSF-based definition. For the “medium” cathode diameter shots, the AWE definition spots are in the range of 2.6-3.1 mm. The “small” cathodes produce spots ~ 2.5 mm and “large” cathodes ~ 3.3 mm. Using our LSF-based definition, the spots are significantly smaller and in the range from 1.8mm-2.7mm for all cathode sizes. The relevance of this comparison between spot definitions as concerns radiographic characterization are two fold. First, the AWE definition based on the ESF has a large contribution associated with the wings of the source distribution, whereas the LSF definition does not. Second, the two definitions would be identical if the source distribution were in fact Gaussian. The fact that the AWE definition value is always larger than the LSF value suggests a more strongly peaked distribution on axis than that of a Gaussian profile. Further it is recognized that the spot measurement as defined by the LSF method results in a more reproducible (shot to shot variation) than the AWE definition, suggesting that the core of the distribution is relatively stable, whereas the wings may be varying more strongly shot to shot. Because of the peaked source distribution, it is reasonable to assume that the source has a larger resolving power than is indicated by the simple spot measurement. A further interesting aspect of the data is the conclusion that for “small” cathode geometries there is the possibility of creating stable sources that can produce ~ 200rads@m, with LSF based spot definition < 2mm.

## IV. Conclusions

Experiments conducted on the RITS-6 accelerator with a low impedance (40  $\Omega$ ) MITL and a Self-Magnetic Pinch diode have demonstrated the capability to create 6.5 MeV endpoint energy bremsstrahlung X-rays with radiation output in excess of 350 rads@m and spot sizes in the range of 2.5-3 mm. This specification meets a near term requirement for scaled core-punch radiography and provides the U.S. with the brightest Pulsed Power driven X-ray source developed to date. The results involved both an optimization of the source geometry and the accelerator to drive the source. The radiographic source figure of merit (FOM), defined as the radiation output divided by the square of the spot-size

$$FOM = \frac{dose}{spot^2} \quad (3)$$

is  $\sim 50$  (rads@m/mm<sup>2</sup>). For comparison, this source is a factor of 15 times brighter than the Cygnus [16] sources, fielded at the Nevada Test Site and only a factor of 2.5 times less bright than the DAHRT 1[17] source at Los Alamos National Labs.

## References

- [1] D. Johnson, et al., "Status of the 10 MV 120 kA RITS-6 inductive voltage adder", Proc. 15<sup>th</sup> IEEE Int. Pulsed Power Conf., Monterrey, Ca., 2005, pp. 314-317.
- [2] I. Smith et al, "Design of a Radiographic Integrated Test Stand (RITS) based on a Voltage Adder, To Drive a Diode Immersed in a High magnetic Field", IEEE Trans. Plasma Sci., Vol 28, No. 5, Oct. 2000, pp. 1653-1659
- [3] J. O'Malley, private communication
- [4] I. Crotch, J. Threadgold, "Self magnetic pinch diode experiments at AWE", in Proc. 14<sup>th</sup> IEEE Int. Pulsed Power Conf., Dig. Tech., Dallas, Texas, June 16-18, 2003, pp. 507-509.
- [5] B.V. Oliver, et al., "Paraxial gas-cell focusing of relativistic electrons for beam radiography", IEEE Trans. Plasma Science, Vol. 33, no. 2, April 2005, pp. 704-711.
- [6] D.C. Rovang, et al., "Operational characteristics and analysis of the immersed-Bz diode on RITS-3", SAND report, SAND2007-0358, February 2007.
- [7] V. L Bailey, et al., "Design of a High Impedance MITL for RITS-3", IEEE pulsed Power Conference proceedings, Dallas, Tx., 2003, pp. 399-402.
- [8] B. V. Oliver, et al., "Two and Three Dimensional MITL Power Flow Studies on Rits", IEEE pulsed Power Conference proceedings, Dallas, Tx., 2003, pp. 395-398.
- [9] C.W. Mendel, et al., Laser Part. Beams, 1, 311, 1983.
- [10] T.J., Goldsack et al., "Multi-megavolt multi-axis high resolution flash X-ray source development", IEEE Trans. Plasma Sci., Vol. 30, 2002, pp. 239-252.
- [11] G. Barnea, et al., "Penumbral imaging made easy", Rev. Sci. Instrum., Vol. 65, No. 6, June 1994, pp. 1949-1953.
- [12] G. Barnea, "SASI – A computer code for megavolt X-ray focal-spot diagnostics", BEAMS 2004, Proc. 15th International Conference on High-Power Particle beams, Saint-Petersburg, Russia, July 18-23, 2004, 577-580; D. V. Efremov Institute (ed. by Gennady Mesyats, Valentin Smirnov and Vladimir Engelco).
- [13] I. Crotch, private communication.

- [14] M.E. Savage, et al., "Time resolved voltage measurements in terawatt magnetically insulated transmission lines", Rev. Sci. Instrum., Vol. 61, No. 12, December 1990, pp. 3812-3820.
  
- [15] D. R. Welch, D. V. Rose, M. E. Cuneo, R. B. Campbell, and T. A. Mehlhorn, Phys. of Plasmas **13**, 063105 (2006); LSP is a software product of ATK Mission Research.
  
- [16] J. Smith, et al., "Cygnus Dual Beam Radiography Source", IEEE pulsed Power Conference proceedings, Monterrey, Ca., 2005, pp. 334,337.
  
- [17] M. J. Burns, et al., 14<sup>th</sup> International Conference on High Power particle Beams, Albuquerque, NM., 2002, pp. 139

## Distribution:

3            Voss Scientific  
              Attn: D. R. Welch  
              D. V. Rose  
              N. Bruner  
              418 Washington SE  
              Albuquerque, NM 87108

3            Naval Research Laboratory  
              Attn: G. Cooperstein (2)  
              D. Hihnshelwood  
              Code 6770  
              4555 Overlook Ave. SW  
              Washington, DC 20375-5346

1            Dept. of Electrical & Computer Engineering  
              Attn: Edl Schamiloglu  
              MSC01 1100  
              1 University of New Mexico  
              Albuquerque, NM 87131-001

10           MS 1193        S. Portillo  
5            MS 1193        B. V. Oliver  
1            MS 1193        J. E. Maenchen  
1            MS 1193        M. D. Johnston  
1            MS 1193        S. R. Cordova  
1            MS 1193        I. Molina  
1            MS 1193        K. D. Hahn  
1            MS 1193        D. L. Johnson  
1            MS 1193        J. J. Leckbee  
1            MS 1193        D. W. Droemer  
1            MS 1193        M. E. Cuneo  
1            MS 1193        J. M. Lehr  
1            MS 1193        D. Ziska  
1            MS 1178        D. M. Van De Valde  
1            MS 1181        T. A. Mehlhorn  
1            MS 1194        M. G. Mazarakis  
1            MS 1194        M. E. Savage  
1            MS 1196        W. A. Stygar  
1            MS 1423        P. A. Miller

2            MS 9018        General Technical Files, 8944  
2            MS 0899        Technical Library, 4336